Journal of Zhejiang University-SCIENCE B 2025 26(12):1245-1259
www.jzus.zju.edu.cn; www.springer.com/journal/11585
E-mail: jzus_b@zju.edu.cn

Research Article
https://doi.org/10.1631/jzus.B2500011

Changes of folate constituents and contents in pakchoi as affected by nitrate to ammonium ratio in nutrient solution under hydroponic conditions

Yongcong ZHU[1], Wei CHENG[1], Yuemin NI[2], Wuzhong NI[1]✉

[1]*Zhejiang Provincial Key Laboratory of Agricultural Resources and Environment, College of Environmental and Resource Sciences, Zhejiang University, Hangzhou 310058, China*
[2]*Agricultural Experimental Station, Zhejiang University, Hangzhou 310058, China*

Abstract: Vegetables are important dietary sources of folate for human nutrition. The influence of different nitrogen doses and forms on changes in primary nitrogen metabolism, such as amino acid and protein synthesis, in plants is well established. However, the impacts of the nitrate-N (NO_3^-)-to-ammonium-N (NH_4^+) ratio on folate synthesis and accumulation in vegetables are unclear. This study used a hydroponic experiment with six different NO_3^-/NH_4^+ ratio treatments to investigate the effects of the integrated application of NO_3^- and NH_4^+ on the folate constituents and contents of pakchoi (*Brassica rapa* subsp. *chinensis*). The results indicated that an appropriate NO_3^-/NH_4^+ ratio in nutrient solution could promote pakchoi growth and increase folate contents by increasing polyglutamylated 5-formyl-tetrahydrofolate (5-CHO-THF) and polyglutamylated 5-methyl-THF (5-CH_3-THF). The activities of enzymes related to folate biosynthesis (except folylpolyglutamate synthase (FPGS)) were lower with an NH_4^+-N supply at the same nitrogen concentration. The statistical results revealed a significant negative correlation between folate contents and 14 detected metabolites (including fructose, sucrose, glutamine (Gln), shikimate, citrate, succinate, malate, α-oxoglutarate, *p*-aminobenzoate (*p*ABA), and 6-hydroxymethyldihydropterin pyrophosphate (HMDH-P_2) in the folate biosynthesis pathway), implying that the enhancement of folates biosynthesis with NH_4^+-N supply increased the consumption of the folate precursors and intermediate metabolites. Additionally, NH_4^+-N supply could improve folate stability by increasing polyglutamylated folates and reducing γ-glutamyl hydrolase (GGH) activity; the latter could weaken folate deglutamylation. As the best growth and highest total folate content were obtained at the appropriate NO_3^-/NH_4^+ ratio, strategic selection of the NO_3^-/NH_4^+ ratio should be considered for the hydroponic cultivation of foliar vegetable crops.

Key words: Pakchoi (*Brassica rapa* subsp. *chinensis*); Nitrate; Ammonium; Folate; Biosynthesis

1 Introduction

Folate (vitamin B9) is the general term for tetrahydrofolate (THF) and its derivatives (folates). Folates play a crucial role in one-carbon (1C) metabolism in living organisms, acting as an enzyme cofactor capable of receiving and donating 1C units. Folates are essential micronutrients for humans that must be obtained through diet due to our lack of ability to synthesize them (Díaz de la Garza et al., 2019). Folate deficiency in the periconceptional period tends to increase the risk of neural tube deformities (NTDs) in infants, and the increased risk of several chronic disorders in humans has also been associated with folate deficiency, including cancer, cardiovascular disease, and neurological conditions (Bailey et al., 2015; US Preventive Services Task Force, 2017). Adequate dietary intake of folates is crucial for human health. The recommended dietary allowance (RDA) for adults is 400 μg/d. For pregnant women, it is 600 μg/d, but not exceeding 1000 μg/d (Bailey, 1998). Synthetic folic acid (FA) has lower bioavailability than natural folate, and excessive intake may have negative health effects (Blancquaert et al., 2014; Scaglione and Panzavolta, 2014). Optimizing folate supply from natural foods is therefore essential.

✉ Wuzhong NI, wzni@zju.edu.cn
Wuzhong NI, https://orcid.org/0000-0002-4367-2697
Yongcong ZHU, https://orcid.org/0000-0002-5388-5979

Received Jan. 7, 2025; Revision accepted Mar. 6, 2025; Crosschecked Dec. 4, 2025

The folate molecule comprises three main components: a *p*-aminobenzoate (*p*ABA) moiety bound to a 2-amino-4-hydroxypteridine (pterin) ring via a carbon (C)-nitrogen (N) bond, linked to a glutamate (Glu) tail via a peptide bond (Fig. 1). THF contains numerous derivatives with different properties, determined by the substituents on N_5 and N_{10}, as well as the length of the Glu tail (Gorelova et al., 2017; Díaz de la Garza et al., 2019). Folates are stabilized through polyglutamylation and accumulate in vacuoles as polyglutamates (Akhtar et al., 2010; Tyagi et al., 2023). Fig. 1 illustrates the metabolic pathway for folate biosynthesis in plants, which can be divided into four parts: precursor synthesis, folate assembly, polyglutamylation and deglutamylation, and transport and distribution (Hanson and Gregory III, 2011; Gorelova et al., 2017). Carbohydrate metabolism is the source of upstream substrates for the folate precursors. These substrates provide chorismate (CHI) for *p*ABA synthesis and supply guanosine triphosphate (GTP) for the conversion to pterin (Fig. 1) (Kołton et al., 2022; Yokoyama et al., 2022).

Currently, crop folate biofortification can be strategically achieved by promoting folate over-synthesis, enhancing its stability and bioavailability via: (1) breeding,

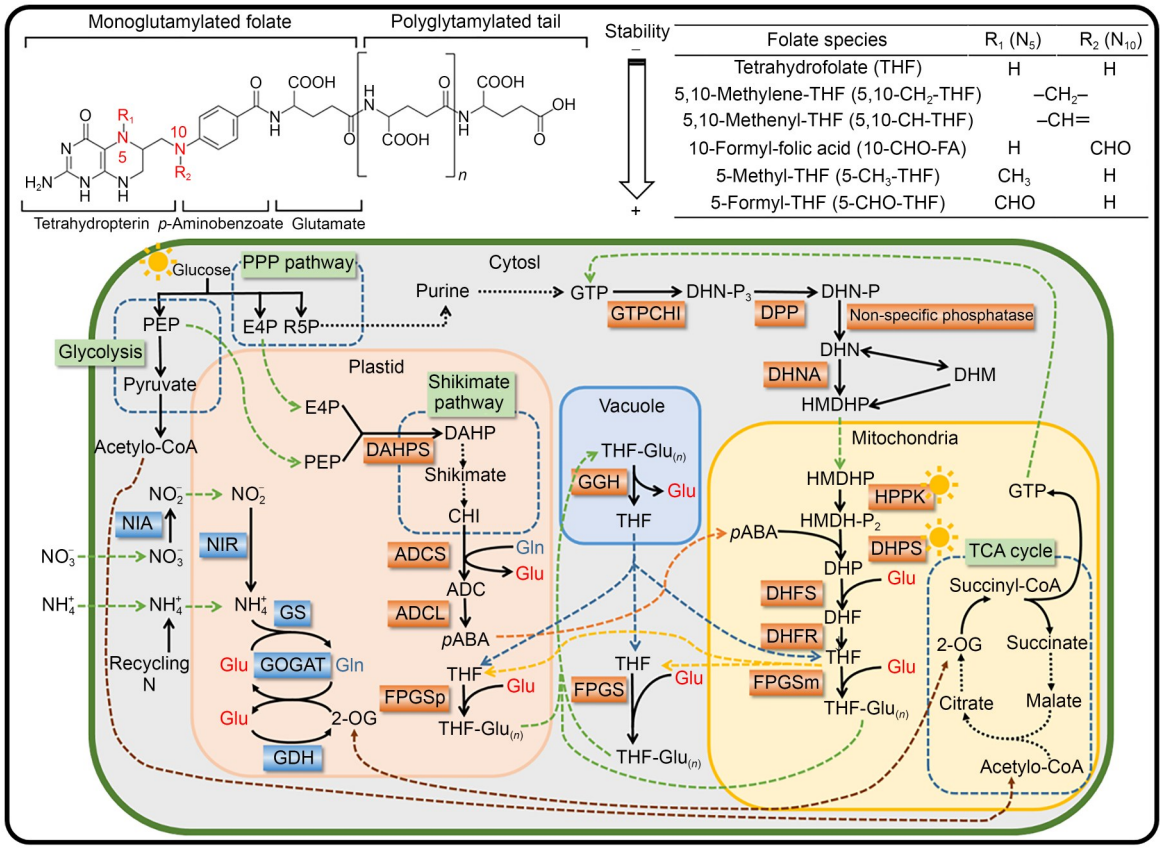

Fig. 1 Folate constituents and their biosynthetic pathways in plants. The two red N indicate the positions of one-carbon groups. R_1 and R_2 represent various one-carbon substituents. Black arrows indicate biosynthetic steps: the solid line indicates the direct step, and the dotted line indicates the indirect step. Non-black dotted arrows indicate transmembrane transport of different substances. PPP: pentose phosphate; TCA: tricarboxylic acid; PEP: phosphoenolpyruvate; E4P: erythrose 4-phosphate; R5P: ribsose-5-phospate; CoA: coenzyme A; NIA: nitrite reductase; NIR: nitrate reductase; Glu: glutamate; Gln: glutamine; GS: Gln synthetase; GOGAT: Gln 2-OG aminotransferase; GDH: Glu dehydrogenase; 2-OG: α-oxoglutarate; DAHP: 3-deoxy-D-arabino-heptulosonate 7-phosphate; DAHPS: DAHP synthase; CHI: chorismate; ADC: aminodeoxychorismate; ADCS: ADC synthase; ADCL: ADC lyase; *p*ABA: *p*-aminobenzoate; GTP: guanosine triphosphate; DHN: dihydroneopterin; DHN-P_3: DHN triphosphate; DHN-P: DHN monophosphate; DPP: DHN triphosphate diphosphatase; DHNA: DHN aldolase; GTPCHI: GTP cyclohydrolase I; DHM: dihydromonapterin; HMDHP: 6-hydroxymethyldihydropterin; HPPK: HMDHP pyrophosphokinase; HMDH-P_2: 6-hydroxymethyldihydropterin pyrophosphate; DHP: dihydropteroate; DHPS: DHP synthase; DHF: dihydrofolate; DHFS: DHF synthase; DHFR: DHF reductase; THF: tetrahydrofolate; THF-$Glu_{(n)}$: THF-polyglutamate; FPGS (m or p): folylpolyglutamate synthase (mitochondrial or plastidial isoform); GGH: γ-glutamyl hydrolase.

(2) metabolic engineering, (3) environmental regulation (light or temperature), (4) chemical elicitation (phytohormones or folate synthesis precursors), and (5) post-harvest processing (Delchier et al., 2016; Saini et al., 2016; Gorelova et al., 2017; Kołton et al., 2022). However, these approaches may face obstacles such as long development cycles, regulation or restriction of transgenic food, additional production costs, and the potential risk of yield reductions. For example, adding Glu and phenylalanine significantly increased the folate content of hydroponically cultivated spinach but reduced its biomass (Watanabe et al., 2017). It is therefore worth exploring universal, inexpensive, and safe means of crop folate biofortification.

N is essential for plant growth and development and is a crucial component of macromolecules such as proteins, nucleic acids, hormones, and vitamins. Plants absorb N in two forms: inorganic N (nitrate-N (NO_3^-) and ammonium-N (NH_4^+)) and organic N (urea, amino acids, and peptides). Inorganic N is the primary form absorbed by plants and the dominant input to agriculture (Krapp, 2015; Liu and von Wirén, 2017; Boschiero et al., 2019). NH_4^+, whether absorbed directly from the outside or converted from NO_3^- reduction, is assimilated into glutamine (Gln) and further converted into Glu (Fig. 1) (Xu et al., 2012). The products Gln and Glu affect folate synthesis and accumulation. Gln acts as an N donor for purine biosynthesis, which is used to produce pterin (Lee et al., 2023). In *p*ABA synthesis, under the catalysis of aminodeoxychorismate (ADC) synthase (ADCS), Gln is hydrolyzed to Glu and NH_4^+, and CHI is converted to ADC using the produced NH_4^+ (Díaz de la Garza et al., 2019; Nakamichi et al., 2023). Glu, the direct synthetic precursor of folate, serves as a tail, the length (the extent of polyglutamylation) of which determines folate stability (Akhtar et al., 2010; Tyagi et al., 2023).

The evidence suggests that NH_4^+ inhibits net NO_3^- uptake, and NO_3^- accelerates net NH_4^+ uptake. Since the coexistence of NO_3^- and NH_4^+ at a specific ratio can overcome the inhibition, plants acquire more N under specific NO_3^-/NH_4^+ ratios, as compared to NO_3^- or NH_4^+ alone (Hachiya and Sakakibara, 2017). Although absorbing NH_4^+ consumes fewer reducing equivalents, excess NH_4^+ can cause toxic action in plants by interfering with energy metabolism and ion uptake and/or disrupting pH balance (Krapp, 2015; Esteban et al., 2016). N assimilation is energetically costly, requiring reducing equivalents and adenosine triphosphate (ATP) and C skeletons, which are initially derived from photosynthate. Specifically, these C skeletons are derived from α-oxoglutarate in the tricarboxylic acid (TCA) cycle (Wang et al., 2014). Exogenous NH_4^+ stimulates cellular NH_4^+ assimilation by bypassing NO_3^- reduction as the rate-limiting step of N assimilation. Compared to sole NO_3^-, more C skeletons are required by the coexistence of NO_3^- and NH_4^+ in response to the increased N assimilation, thus enhancing C input to the TCA cycle (Hachiya and Sakakibara, 2017).

N supply is essential for folate synthesis, including its availability and forms, and its sufficiency is critical for folate synthesis; lower folate content is exhibited under N deficiency (Wang et al., 2023). Plants' N acquisition and N assimilation change under different NO_3^-/NH_4^+ ratios, thus altering Glu and Gln contents; however, the effect of these changes on folate content has not yet been explored. The substrates of folate biosynthesis precursors and the C skeletons for N assimilation are both derived from the C metabolism of glycolysis (Wang et al., 2014; Kołton et al., 2022). One study indicated that folate accumulation can be controlled by pyruvate metabolism in glycolysis (Lian et al., 2022). Whether folate biosynthesis is regulated by changes in C and N metabolism induced by different NO_3^-/NH_4^+ ratios remains poorly understood. Additionally, vegetables in soilless culture rarely use NH_4^+-N as a source of N. Thus, we chose a folate-rich, leafy vegetable, pakchoi (*Brassica rapa* subsp. *chinensis*), as the experimental material, and through hydroponic experiments, we studied the effect of N with different NO_3^-/NH_4^+ ratios on folate biosynthesis and accumulation. The results of this study can inform folate enhancement strategies with reasonable nitrogen fertilization.

2 Materials and methods

2.1 Hydroponic experiment and plant sampling

Pakchoi (*B. rapa* subsp. *chinensis*) seeds (II2B8210) were used for this study. Seeds were surface sterilized by soaking in 2% H_2O_2 for 10 min and fully rinsed with deionized water. Subsequently, the seeds were soaked in deionized water for 24 h in the dark and then germinated in a moist sand substrate. After 10 d, healthy seedlings of a similar size were selected and

cultured in pots containing 4 L of nutrient solutions (Table 1) in an aerated medium. We prepared six nutrient solutions with different NO_3^-/NH_4^+ ratios (100/0, 90/10, 80/20, 70/30, 60/40, and 50/50) at a 15 mmol/L N concentration. After transplanting, all plants were cultured over three periods: for the first 6 d in the 100/0-ratio nutrient solution with 25% ionic strength, then up to 50% ionic strength for 6 d, and finally in the complete (100% ionic strength) nutrient solution for 6 d. Next, all plants were randomly divided into six groups, each cultured in one of the six different complete nutrient solutions for 12 d. The experiment was performed in controlled environmental conditions: temperature ((25±5) ℃), photoperiod (light/dark cycle, 12 h/12 h), relative humidity ((55±5)%), pH of all nutrient solutions (adjusted to 5.8 before application), and renewal of all nutrient solutions (every 3 d throughout the experiment). Pots were randomly placed with three replicates per treatment, and eight plants were hydroponically grown in each pot.

Table 1 Nitrogen, phosphorus, and potassium concentrations of the nutrient solution with different NO_3^-/NH_4^+ ratios

NO_3^-/NH_4^+ ratio	Nutrient concentration (mmol/L)				
	NO_3^--N	NH_4^+-N	Total-N	P	K
100/0	15.0	0.0	15.0	1.0	6.0
90/10	13.5	1.5	15.0	1.0	6.0
80/20	12.0	3.0	15.0	1.0	6.0
70/30	10.5	4.5	15.0	1.0	6.0
60/40	9.0	6.0	15.0	1.0	6.0
50/50	7.5	7.5	15.0	1.0	6.0

Micronutrients were supplied at the following concentrations: 5 mmol/L Ca; 2 mmol/L Mg; 0.1 mmol/L Fe; 0.01 mmol/L Mn; 0.001 mmol/L Cu; 0.001 mmol/L Zn; 0.033 mmol/L B; 0.002 mmol/L Mo.

After culturing for 30 d to reach commercial maturity, the plants were harvested, and the fresh weights were measured. Subsequently, the fresh edible tissues were washed with deionized water and then dried with absorbent paper. The first part was immediately placed into liquid nitrogen and then cryogenically homogenized into fine powder and stored at −80 ℃ before undergoing metabolite and enzyme activity analysis. Another part was oven-dried at 105 ℃ for 30 min, and then at 60 ℃ to a constant weight, before being ground into a fine powder for element determination.

2.2 Folate extraction and quantification

Folate was extracted using tri-enzyme (α-amylase, protease, and γ-glutamyl hydrolase (GGH)) treatment without light, as described in a previous study with some modifications (He et al., 2022). Briefly, a 0.2 g cryogenically stored sample was added to a 2.0 mL brown capped tube with 1 mL extraction buffer (50 mmol/L phosphate buffer containing 1% (volume fraction) L-ascorbic acid and 0.1% (volume fraction) 2-mercaptoethanol, pH 7.2; freshly prepared). After mixing, the tube was placed at 100 ℃ for 5 min and flash-cooled on ice at room temperature, preventing the conversion metabolism of folate derivatives. To capture potential folates in carbohydrates and proteins, the extract was treated with α-amylase and papain. After being mixed with 50 μL of α-amylase (20 mg/mL), the extract was incubated at 37 ℃ for 30 min under vibration. Subsequently, 100 μL of papain (20 mg/mL), a protease, was added, and then the sample was incubated at 37 ℃ for 1 h under vibration. The sample was placed at 100 ℃ for 5 min to denature the enzyme, then flash-cooled on ice at room temperature. After centrifuging at 12 000*g*, 4 ℃ for 20 min, the supernatant was collected. The most common sources of GGHs for folate analysis are rat plasma, hog kidney, and chicken pancreas extracts (Ramos-Parra et al., 2013). Next, 500 μL supernatant was mixed with 100 μL rat serum and incubated at 37 ℃ for 4 h under vibration to deconjugate polyglutamylated folates. To eliminate the effect of endogenous folates on the quantification, the rat serum was mixed with activated charcoal (1:10, mass/volume), centrifuged after an ice bath for 1 h, and then filtered before folate deconjugation. After repeating the enzyme denaturation and cooling steps, the sample was centrifuged at 12 000*g*, 4 ℃ for 20 min, and then filtered through a 0.45 μm nylon membrane filter into a 2 mL brown vial for quantification.

To quantify monoglutamylated folate (MG) and polyglutamylated folate (PG), the extraction followed the same steps as the folates, except that the step of rat serum treatment was omitted. MG was the quantified value without GGH treatment. PG was calculated by subtracting the MG from the value quantified in the deglutamylated sample, indicated by the equation below (Ramos-Parra et al., 2013):

$$PG = MG_{GGH\text{-}treated} - MG_{non\text{-}treated}.$$

The sample was introduced into the ultra-high performance liquid chromotography (UHPLC) system (Acquity UHPLC M-Class system, Waters, USA)-triple quadruple mass spectrometry (MS) (Xevo TQ-S,

Waters, USA) for mass analyses and quantification according to the previous liquid chromatography-tandem MS (LC-MS/MS) settings with some modifications (Wan et al., 2019). The sample was separated using an Acquity UPLC BEH-C18 column (Waters, 2.1 mm×100 mm, 1.7 μm) at a flow rate of 0.35 mL/min. The injection volume was 1.2 μL at 4 ℃, and the column temperature was set at 30 ℃. The mobile phases were 0.1% (volume fraction) formic acid in water (phase A) and 0.1% (volume fraction) formic acid in acetonitrile (phase B). The gradient program lasted a total of 6 min: initiated with 10% B (volume fraction, the same below) with a 0.5 min hold, increased to 50% over 0.7 min, and then increased to 95% over 1.8 min. After holding at 95% for 1 min, it immediately adjusted to its initial composition over 0.2 min, followed by an equilibration time of 1.8 min. The mass spectrometer was operated in positive ion mode. The parameters were optimized for folate analysis with a capillary voltage of 3160 V, desolvation temperature of 350 ℃, desolvation gas flow of 800 L/h, cone gas flow of 152 L/h, collision gas flow of 0.12 mL/min, and nebulizer pressure of 0.7 MPa. Data were acquired in the optimized multiple reaction monitoring (MRM) mode (Table 2). Using external folate standards, the folate concentrations were calculated from the calibration curve. The commercial folate standards (FA HPLC≥ 98%; THF HPLC=65%; 10-formyl-FA (10-CHO-FA) HPLC≥95%; 5-methyl-THF (5-CH_3-THF) HPLC≥ 98%; 5-formyl-THF (5-CHO-THF) HPLC≥98%) were purchased from Shanghai Yuanye Bio-Technology Co., Ltd., China.

2.3 Metabolites extraction and determination

The metabolite extraction was performed using a method similar to that described by Gao et al. (2023). The cryogenically stored sample was extracted using the same extraction buffer as that used for folate extraction, then centrifuged at 1000*g* and 4 ℃ for 20 min, and the supernatant was collected. To detect the metabolites (CHI, ADC, *p*ABA, GTP, dihydroneopterin triphosphate (DHN-P_3), 6-hydroxymethyldihydropterin (HMDHP), 6-hydroxymethyldihydropterin pyrophosphate (HMDH-P_2), dihydropteroate (DHP), dihydrofolate (DHF), Glu, Gln, and folate-binding protein (FBP)), the supernatant was treated with the plant-specific enzyme-linked immunosorbent assay (ELISA) kits (Shanghai Enzyme-linked Biotechnology Co., Ltd., China) according to the manufacturer's instructions. The content of each metabolite was calculated as the fresh weight (FW).

For the analysis of sugar components (glucose, fructose, and sucrose), 0.3 g of cryogenically stored sample and 2 mL of ultrapure water (autoclaved before use) were mixed, and then extracted at 100 ℃ for 20 min. After cooling and centrifugation, the supernatant was collected and then filtered for injection into the HPLC (Waters 2695, USA) coupled with a refractive index (RI) detector. The sample was separated using an amino (NH_2) column (Waters, 3.9 mm×300 mm, 10 μm). The injection volume was 10 μL, and the column temperature was set at 80 ℃. The mobile phase was the ultrapure water at a flow rate of 0.6 mL/min.

For the analysis of organic acid components (pyruvate, shikimate, citrate, succinate, malate, and α-oxoglutarate), 0.3 g of cryogenically stored sample and 2 mL of 2 g/L metaphosphate buffer solution were mixed, and then extracted with an ice bath for 10 min. After centrifugation at 4 ℃, the supernatant was collected and then filtered for injection into the HPLC (Waters 2695, USA) coupled with an ultraviolet-visible (UV-Vis) detector. The sample was separated using an XSelect HSS T3 Column (Waters, 4.6 mm×250 mm, 3.5 μm). The injection volume was 10 μL, and the column temperature was set at 35 ℃. The mobile phase was the 0.2% (volume fraction) metaphosphate buffer (filtered through a 0.45 μm filter) at a flow rate of 1 mL/min.

Table 2 Tandem mass spectrometry-multiple reaction monitoring (MS/MS-MRM) parameters and retention time of five folate species

Folate analyte	Precursor ion (*m/z*)	Product ion (*m/z*)	Cone energy (V)	Collision energy (V)
FA	442.1	295.1	30.0	14.0
THF	446.1	299.1	30.0	20.0
10-CHO-FA	470.3	294.9	40.0	24.0
5-CH_3-THF	460.2	313.1	20.0	18.0
5-CHO-THF	474.2	327.1	29.0	18.0

FA: folic acid; THF: tetrahydrofolate; 10-CHO-FA: 10-formyl-FA; 5-CH_3-THF: 5-methyl-THF; 5-CHO-THF: 5-formyl-THF.

2.4 Enzyme extraction and activity determination

The enzyme extraction was performed using the same method as that used for metabolite extraction. To detect enzyme activities (3-deoxy-D-arabino-heptulosonate 7-phosphate synthase (DAHPS), ADCS, ADC lyase (ADCL), GTP cyclohydrolase I (GTPCHI), HMDHP pyrophosphokinase-DHP synthase (HPPK-DHPS), DHF synthase (DHFS), DHF reductase (DHFR), folylpolyglutamate synthase (FPGS), and GGH), the supernatant was treated with the plant-specific ELISA kits purchased from Shanghai Enzyme-linked Biotechnology according to the manufacturer's instructions. The units of enzyme activity per gram fresh weight (FW) were abbreviated as U/g FW, according to the kit instructions.

2.5 Statistical analysis

Three independent biological replicates were used for all tests. All the data were collated and analyzed for basic statistics using Microsoft Excel. One-way analysis of variance (ANOVA), followed by multiple comparisons with Duncan's (P<0.05), was also performed using SAS 9.2. Correlation analysis was performed using IBM SPSS Statistics 20, and heatmaps of the correlation analyses were generated using ChiPlot (https://www.chiplot.online).

3 Results

3.1 Fresh weights of different NO_3^-/NH_4^+ ratio treatments

Root and whole plant fresh weights of the treatments with NH_4^+-N (90/10 to 50/50 NO_3^-/NH_4^+ ratio) were significantly higher than those of the control (100/0 NO_3^-/NH_4^+ ratio) (Table 3). Shoot fresh weights of treatments with NH_4^+-N were at least 2% higher than those of the control (though not significant). The treatment with a 70/30 NO_3^-/NH_4^+ ratio was the best. NH_4^+ did not inhibit the growth of pakchoi (a NO_3^--preferred vegetable crop) at the same N concentration, even with a 50/50 NO_3^-/NH_4^+ ratio.

3.2 Folate constituents and contents of different NO_3^-/NH_4^+ ratio treatments

As shown in Fig. 2a, the total folate contents in pakchoi shoots with NH_4^+-N treatments were significantly higher, approximately 1.3-fold to 1.5-fold, than those of the 100/0 NO_3^-/NH_4^+ ratio treatment ((151.2±17.6) μg/100 g FW). The treatment with a 70/30 NO_3^-/NH_4^+ ratio was the best for increasing total folate contents ((231.7±15.0) μg/100 g FW). Among five detected folate vitamers, the FA contents of 70/30, 60/40, and 50/50 NO_3^-/NH_4^+ ratio treatments were significantly higher than that of the 100/0 NO_3^-/NH_4^+ ratio treatment. The 5-CH_3-THF, 5-CHO-THF, and 10-CHO-FA contents of all five treatments with NH_4^+-N were significantly higher than those of the 100/0 NO_3^-/NH_4^+ ratio treatment, whereas the differences in THF contents among all six treatments were not significant. The treatment with the 70/30 NO_3^-/NH_4^+ ratio was the best for increasing the contents of FA, 5-CH_3-THF, 5-CHO-THF, and 10-CHO-FA (the specific folate contents are provided in Table S1).

Table 3 Pakchoi fresh weights of different NO_3^-/NH_4^+ ratio treatments

NO_3^-/NH_4^+ ratio	Fresh weight (g/plant)		
	Shoot	Root	Whole plant
100/0	8.98±0.52^a	0.59±0.02^d	9.58±0.51^c
90/10	9.14±0.83^a	0.73±0.04^c	9.87±0.87^b
80/20	9.33±0.42^a	0.91±0.03^b	10.24±0.42^{ab}
70/30	9.98±0.10^a	1.00±0.02^a	10.98±0.12^a
60/40	9.23±0.26^a	0.89±0.04^b	10.12±0.24^{ab}
50/50	9.21±0.25^a	0.73±0.02^c	9.94±0.24^b

The biomass of the whole plant is equal to the sum of root (underground) and shoot (aboveground) biomass. Data are the mean values per plant and are expressed as mean±standard deviation (SD), n=3. Different letters indicate significant difference among treatments according to Duncan's test (P<0.05).

As shown in Fig. 2b, the MG FA contents of the treatments with 70/30, 60/40, and 50/50 NO_3^-/NH_4^+ ratios were significantly higher than those of the 100/0 NO_3^-/NH_4^+ ratio treatment, as were the treatments with 70/30 and 60/40 NO_3^-/NH_4^+ ratios with respect to MG THF contents. As shown in Fig. 2c, the PG FA, PG 5-CH_3-THF, and PG 5-CHO-THF contents of the treatments with 70/30, 60/40, and 50/50 NO_3^-/NH_4^+ ratios were significantly higher than those of the 100/0 NO_3^-/NH_4^+ ratio treatment. The PG 10-CHO-FA contents of all five treatments with NH_4^+-N were significantly higher than those of the 100/0 NO_3^-/NH_4^+ ratio treatment.

It was also found that the higher 5-CHO-THF (36%), 5-CH_3-THF (32%), and FA (20%) mainly contributed to the highest total folate contents of the treatment with a 70/30 NO_3^-/NH_4^+ ratio. Increases in

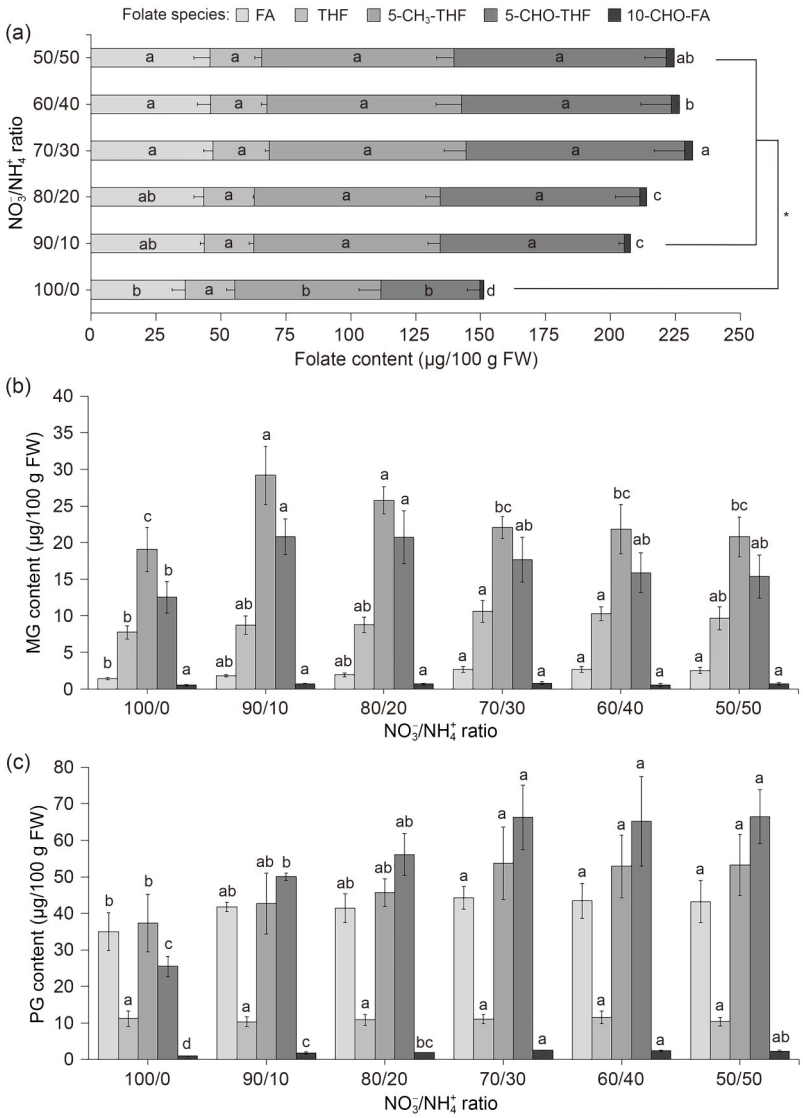

Fig. 2 Folate constituents and contents in pachoi fresh shoots hydroponically cultivated at different NO_3^-/NH_4^+ ratios. (a) Total folates and five folate vitamers, viz. folic acid (FA), tetrahydrofolate (THF), 5-methyl-THF (5-CH_3-THF), 5-formyl-THF (5-CHO-THF), and 10-formyl-FA (10-CHO-FA), were analyzed from the fresh shoots of pakchoi. (b) Monoglutamylated folate (MG) contents. (c) Polyglutamylated folate (PG) contents. FW: fresh weight. Data are expressed as mean±standard deviation (SD), *n*=3. The different letters indicate significant differences among treatments according to Duncan's test (*P*< 0.05). In (a), an asterisk (*) shows a significant difference in total folate contents (*P*<0.05) between the treatment groups.

5-CHO-THF and 5-CH_3-THF were exhibited with the higher PG 5-CHO-THF and PG 5-CH_3-THF, respectively. The FA contents increased with the higher MG FA and PG FA contents. In general, total folate contents increased with both the higher PG 5-CHO-THF and PG 5-CH_3-THF.

3.3 Activities of enzymes affected by different NO_3^-/NH_4^+ ratio treatments

The activities of nine enzymes related to folate biosynthesis, such as GTPCHI, DAHPS, ADCS, ADCL, HPPK-DHPS, DHFS, DHFR, FPGS, and GGH, were analyzed. As shown in Fig. 3, the activities of GTPCHI, DHFS, DHFR, and GGH in pakchoi shoots after the five treatments with NH_4^+-N were significantly lower than those after the 100/0 NO_3^-/NH_4^+ ratio treatment, and the ADCS activities of the treatments with 90/10, 80/20, and 50/50 NO_3^-/NH_4^+ ratios were also significantly lower than that of the 100/0 NO_3^-/NH_4^+ ratio treatment. The activities of DAHPS, ACDL, and HPPK-DHPS of all six treatments were similar, except for the 50/50 NO_3^-/NH_4^+ ratio treatment for DAHPS and ACDL activities,

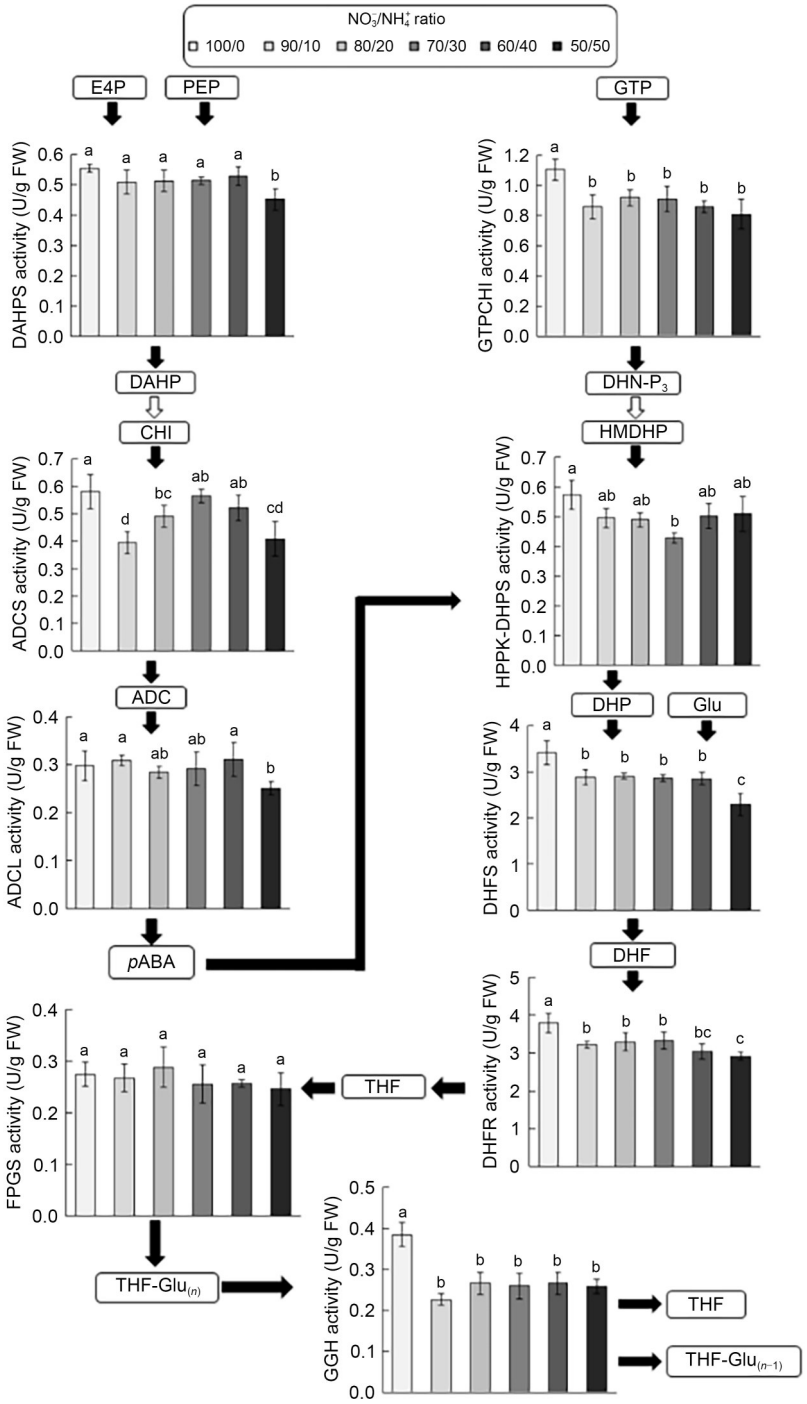

Fig. 3 Changes in the activities of enzymes related to folate biosynthesis in pakchoi shoots among different NO_3^-/NH_4^+ ratio treatments. The black arrow represents the direct conversion process, and the white arrow represents the multi-step conversion process. FW: fresh weight; E4P: erythrose 4-phosphate; PEP: phosphoenolpyruvate; DAHP: 3-deoxy-D-arabino-heptulosonate 7-phosphate; DAHPS: DAHP synthase; CHI: chorismite; ADC: aminodeoxychorismate; ADCS: ADC synthase; ADCL: ADC lyase; *p*ABA: *p*-aminobenzoate; GTP: guanosine triphosphate; GTPCHI: GTP cyclohydrolase I; DHN-P_3: dihydroneopterin triphosphate; HMDHP: 6-hydroxymethyldihydropterin; DHP: dihydropteroate; HPPK-DHPS: HMDHP pyrophosphokinase-DHP synthase; DHF: dihydrofolate; DHFS: DHF synthase; DHFR: DHF reductase; THF: tetrahydrofolate; THF-$Glu_{(n)}$: THF-polyglutamate; Glu: glutamate; FPGS: folylpolyglutamate synthase; GGH: γ-glutamyl hydrolase. Data are expressed as mean±standard deviation (SD), *n*=3. The different letters indicate significant differences among treatments according to Duncan's test (*P*<0.05).

and the 70/30 NO_3^-/NH_4^+ ratio treatment for HPPK-DHPS activity. The differences in FPGS activities among all six treatments were not significant (the specific activities of the enzymes are provided in Table S1).

3.4 Changes of metabolites in folate biosynthesis with different NO_3^-/NH_4^+ ratio treatments

The biosynthesis of folates in plants is based on substances derived from carbon metabolism. Thus, the primary metabolites of carbon metabolism, such as sugars and organic acids in pakchoi shoots, were analyzed. As shown in Fig. 4, the glucose contents of the five treatments with NH_4^+-N were significantly higher than that of the 100/0 NO_3^-/NH_4^+ treatment, as the sucrose and fructose contents decreased significantly, except for the sucrose content after the 90/10 NO_3^-/NH_4^+ ratio treatment. The pyruvate and shikimate contents of the five treatments with NH_4^+-N were significantly lower than those of the 100/0 NO_3^-/NH_4^+ treatment, except for the 90/10 NO_3^-/NH_4^+ ratio treatment. Citrate, malate, α-oxoglutarate, and succinate contents of the five treatments with NH_4^+-N were also significantly lower than those of the 100/0 NO_3^-/NH_4^+ treatment, except for the 90/10 NO_3^-/NH_4^+ ratio treatment for malate and succinate contents (the specific metabolite contents are provided in Table S1).

Glu and Gln, the products of N assimilation involved in folate synthesis in pakchoi shoots, were analyzed (Fig. 4). The Gln contents of all five treatments with NH_4^+-N were significantly lower than that of the 100/0 NO_3^-/NH_4^+ treatment, and the Glu contents of the treatments with 90/10, 80/20 and 50/50 NO_3^-/NH_4^+ ratios were also significantly lower than that of the 100/0 NO_3^-/NH_4^+ treatment.

To examine the impacts of NO_3^--N and NH_4^+-N supply on folate accumulation in pakchoi shoots, the intermediate metabolites such as CHI, ADC, *p*ABA, GTP, DHN-P_3, HMDHP, HMDH-P_2, DHP, and DHF in the folate synthesis pathway were analyzed. As shown in Fig. 4, in the *p*ABA synthesis section, the contents of CHI, ADC, and *p*ABA of all five treatments with NH_4^+-N were significantly lower than those of the 100/0 NO_3^-/NH_4^+ treatment. In the HMDH-P_2 synthesis section, the contents of GTP, DHN-P_3, HMDHP, and HMDH-P_2 of five treatments with NH_4^+-N were significantly lower than those of the 100/0 NO_3^-/NH_4^+ treatment except for the 70/30 NO_3^-/NH_4^+ ratio treatment for GTP and DHN-P_3 contents. In the folate assembly section, only the 50/50 NO_3^-/NH_4^+ ratio treatment had significantly lower DHP contents than the 100/0 NO_3^-/NH_4^+ treatment, and the differences in DHF contents among all six treatments were not significant.

FBP, a protein with folate-binding ability, can improve folate stability and contribute to folate accumulation (Blancquaert et al., 2015). FBP was analyzed to examine the impacts of NO_3^--N and NH_4^+-N supply on FBP in pakchoi shoots. As shown in Fig. 4, FBP contents did not vary significantly among all six treatments.

3.5 Correlations of enzyme activities and folates with metabolites

The correlations of enzyme activities with corresponding metabolites are presented in Fig. 5a. The GTPCHI, ADCS, HPPK-DHPS, and DHFS activities were significantly positively correlated with their corresponding substrate, such as (1) GTP, (2) chorismate, (3) *p*ABA, HMDHP, and HMDH-P_2, and (4) DHP and Glu. The consequential products, ADC, Glu, and DHP, were significantly positively correlated with their corresponding enzyme activity. Total folate contents were significantly negatively correlated with both DHFR and GGH activities.

The correlations of folates with 21 metabolites are shown in Fig. 5b. FA, THF, 5-CH_3-THF, 5-CHO-THF, 10-CHO-FA, and total folates were significantly positively correlated with glucose (the initial metabolite). Negative correlations were demonstrated among total folates or between each folate form and 20 other metabolites, even significant associations, such as FA with 10 metabolites (fructose, sucrose, shikimate, citrate, succinate, malate, α-oxoglutarate, *p*ABA, HMDH-P_2, and Gln); THF with one metabolite (*p*ABA); 5-CH_3-THF with 12 metabolites (fructose, sucrose, shikimate, citrate, succinate, malate, α-oxoglutarate, chorismite, ADC, *p*ABA, HMDH-P_2, and Gln); and 5-CHO-THF, 10-CHO-THF, and total folates each with 14 metabolites (fructose, sucrose, pyruvate, shikimate, citrate, succinate, malate, α-oxoglutarate, chorismite, ADC, *p*ABA, HMDH-P_2, DHP, and Gln).

4 Discussion

Our research revealed that simply optimizing NO_3^-/NH_4^+ ratio leads to a 1.5-fold increase in folate level (231.7 μg/100 g FW) in fresh shoots of hydroponically

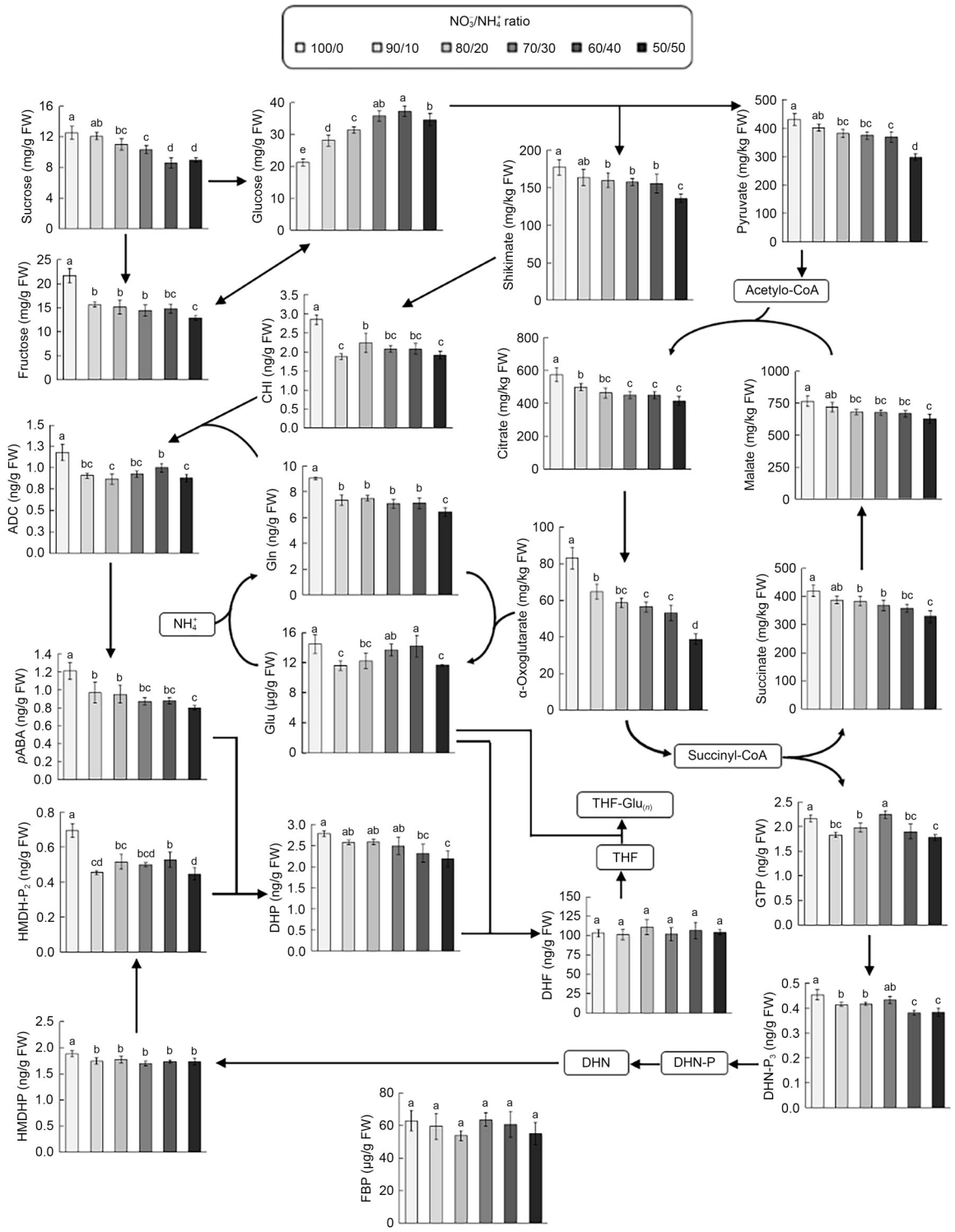

Fig. 4 Changes in the metabolic profiles in the pakchoi shoots among different NO_3^-/NH_4^+ ratio treatments. FW: fresh weight; CHI: chorismite; ADC: aminodeoxychorismate; *p*ABA: *p*-aminobenzoate; Gln: glutamine; Glu: glutamate; DHP: dihydropteroate; HMDHP: 6-hydroxymethyldihydropterin; HMDH-P_2: HMDHP pyrophosphate; GTP: guanosine triphosphate; DHN: dihydroneopterin; DHN-P_3: DHN triphosphate; DHN-P: DHN monophosphate; DHF: dihydrofolate; THF: tetrahydrofolate; THF-$Glu_{(n)}$: THF-polyglutamate; FBP: folate-binding protein. Data are expressed as mean±standard deviation (SD), *n*=3. Different letters indicate significant differences among treatments according to Duncan's test ($P<0.05$).

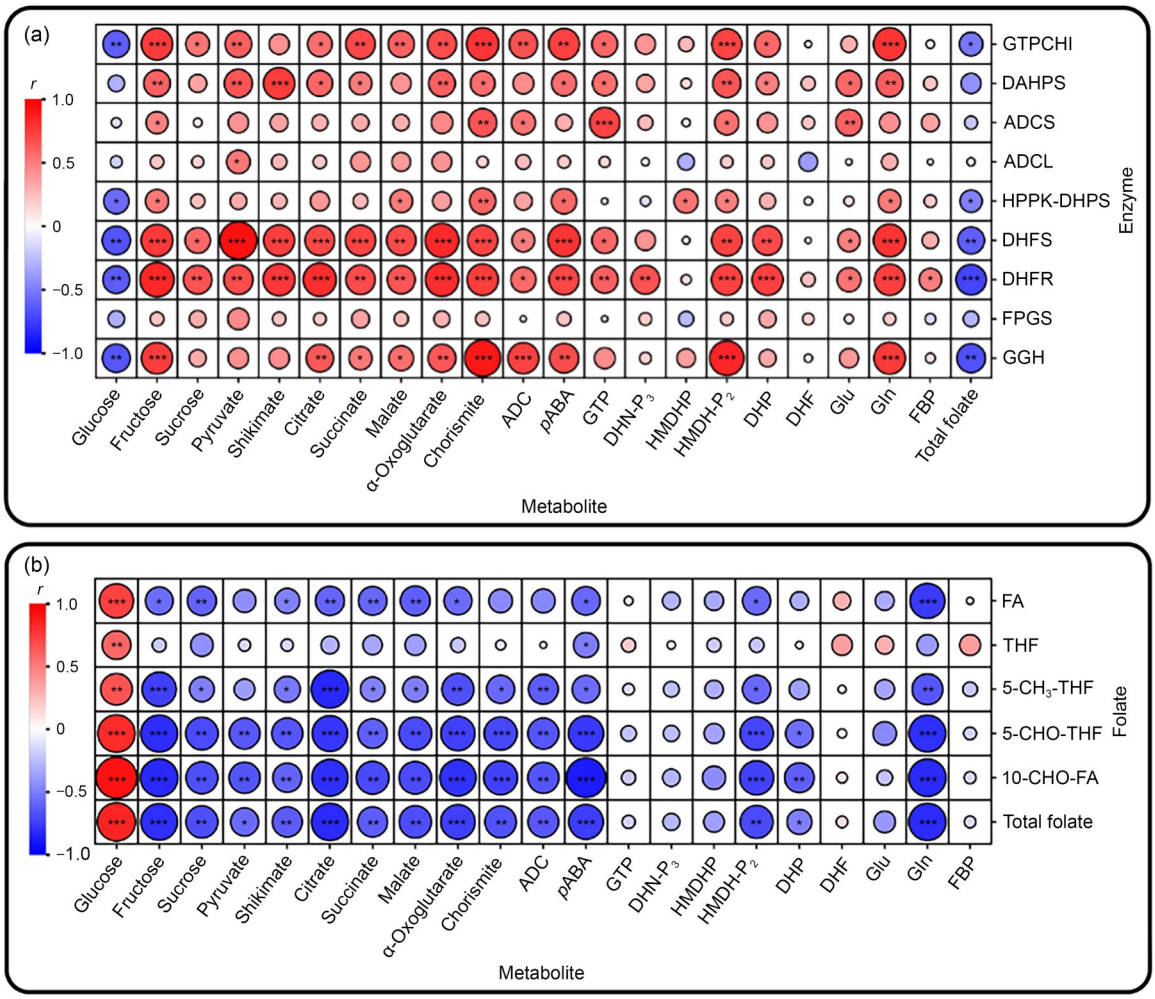

Fig. 5 Heatmaps of correlations between enzyme activities, folates, and metabolites. (a) Correlations between enzyme activities and metabolites. (b) Correlations between folates and metabolites. Correlation analyses of all metabolite contents and enzyme activities were based on fresh weight (FW). Correlations were calculated using Pearson's coefficients (*r*). The size of the circle indicates the degree of the correlation. Positive correlations are red, and negative correlations are blue. * *P*<0.05, ** *P*<0.01, and * *P*<0.001. FA: folic acid; THF: tetrahydrofolate; 5-CH_3-THF: 5-methyl-THF; 5-CHO-THF: 5-formyl-THF; 10-CHO-FA: 10-formyl-FA; ADC: aminodeoxychorismate; *p*ABA: *p*-aminobenzoate; GTP: guanosine triphosphate; DHN-P_3: dihydroneopterin (DHN) triphosphate; HMDHP: 6-hydroxymethyldihydropterin; HMDH-P_2: HMDHP pyrophosphate; DHP: dihydropteroate; DHF: dihydrofolate; Glu: glutamate; Gln: glutamine; FBP: folate-binding protein; DAHPS: 3-deoxy-D-arabino-heptulosonate 7-phosphate synthase; ADCS: ADC synthase; ADCL: ADC lyase; GTPCHI: GTP cyclohydrolase I; HPPK-DHPS: HMDHP pyrophosphokinase-DHP synthase; DHFS: DHF synthase; DHFR: DHF reductase; FPGS: folylpolyglutamate synthase; GGH: γ-glutamyl hydrolase.**

cultivated pakchoi, with a 70/30 NO_3^-/NH_4^+ ratio treatment producing the best growth compared to no NH_4^+-N treatment. The higher folate level with the 70/30 NO_3^-/NH_4^+ ratio may reflect a higher rate of folate biosynthesis or a reduction in folate degradation. We speculate that the appropriate (70/30) NO_3^-/NH_4^+ ratio induces folate enrichment for the following reasons.

First, an appropriate NO_3^-/NH_4^+ ratio could stimulate C metabolism to provide additional material support for folate biosynthesis. GTP and CHI, both required for folate biosynthesis, are derived from C metabolism. Carbohydrates can be converted into GTP via glycolysis through the TCA cycle or into CHI via glycolysis through the shikimate pathway (Kołton et al., 2022). Additionally, the C skeletons that are required for the biosynthesis of Glu and Gln, which are essential for folate synthesis, are derived from α-oxoglutarate in the TCA cycle (Wang et al., 2014). C input to the TCA cycle via the glycolysis through pyruvate kinase was enhanced when both NO_3^--N and NH_4^+-N supplies were

present compared with NO_3^--N supply alone (Hachiya and Sakakibara, 2017). In our study, the low levels of pyruvate in the glycolysis and the low levels of citrate, succinate, malate, and α-oxoglutarate in the TCA cycle of the treatments with NH_4^+-N may be responsible for the enhanced C fluxes, providing more C skeletons for N assimilation. Fructose requires fewer catalytic steps than glucose to enter glycolysis (Patrick et al., 2013). The low fructose levels may reflect more efficient utilization for enhancing C metabolism with NH_4^+-N application. Since sucrose is formed by glucose and fructose, the decreased sucrose level may result from accelerated fructose consumption. It seems reasonable that with the addition of NH_4^+-N, a low GTP level was observed due to the enhanced GTP consumption for folate biosynthesis; as the NO_3^-/NH_4^+ ratio declined, the GTP level increased due to the increased output from the TCA cycle.

However, excessive NH_4^+-N may weaken photosynthesis, thereby reducing C metabolism input (Esteban et al., 2016). With an excessively low NO_3^-/NH_4^+ ratio (e.g., 50/50 NO_3^-/NH_4^+), the GTP level decreased due to the lower C input to the TCA cycle and the lower α-oxoglutarate level. As with GTP, low chorismite levels in the treatments with NH_4^+-N may result from enhanced chorismite consumption due to increased folate biosynthesis. DAHPS catalyzes the first step of enzymatic reactions in the shikimate pathway (Yokoyama et al., 2022). In our study, low DAHPS activity at the 50/50 NO_3^-/NH_4^+ ratio may limit the C flux into the shikimate pathway. Excessive NH_4^+ can also enhance the anaplerotic routes for greater C input to the TCA cycle through pyruvate kinase (Esteban et al., 2016). Low CHI level at the 50/50 NO_3^-/NH_4^+ ratio may also be a response to the decreased shikimate caused by the reduced C flux input and/or the additional C redirected to the TCA cycle. Overall, this evidence suggests that an appropriate NO_3^-/NH_4^+ ratio enhanced C metabolism to promote fluxes for folate synthesis.

Second, an appropriate NO_3^-/NH_4^+ ratio could stimulate the conversion of GTP to HMDHP via a series of steps. The GTPCHI catalyzes a net expansion of the GTP to form a pteridine derivative, DHN-P_3, which represents a rate-limiting step controlling metabolic flux into the folate biosynthesis pathway (Gräwert et al., 2013; Gorelova et al., 2017). In our study, folate content increased with the addition of NH_4^+-N, despite the reduced GTPCHI activity. This reduction in GTPCHI activity is more likely to be attributable to negative feedback regulation by the enhanced metabolism. In pakchoi, folate levels were elevated by controlled illumination, which is attributed to decreased GTP and HMDHP levels (Gao et al., 2023). Similarly, with the addition of NH_4^+-N, low GTP, DHN-P_3, and HMDHP levels may be the result of their greater consumption for folate biosynthesis.

Third, an appropriate NO_3^-/NH_4^+ ratio could also stimulate the conversion of CHI to *p*ABA. *p*ABA biosynthesis starts with CHI by catalyzing two reactions: NH_4^+ release from Gln and hydroxyl group replacement with the amino group yielding ADC (Díaz de la Garza et al., 2019). In our study, the levels of CHI, ADC, *p*ABA, and Gln decreased with the addition of NH_4^+-N due to the enhanced folate biosynthesis, which consumed more of them. Folate levels in the pakchoi were elevated by controlled illumination, which is attributed to the decreased CHI and ADC levels (Gao et al., 2023). This evidence supports that the decline of *p*ABA resulted from the enhanced folate biosynthesis in our study.

Additionally, an appropriate NO_3^-/NH_4^+ ratio could promote folate assembly. Folate is produced in mitochondria, where HMDHP is phosphorylated by HPPK to form HMDH-P_2, and this moiety is condensed with *p*ABA to form DHP by DHPS. DHP is then glutamylated by DHFS to form DHF, which is further reduced to THF by DHFR (Gorelova et al., 2017). In our study, the low HMDH-P_2 and DHP levels associated with the addition of NH_4^+-N may be the result of the promotion of folate biosynthesis. Notably, high folate levels at 70/30 and 60/40 NO_3^-/NH_4^+ ratios may be attributed to high Glu level because Glu acts as a donor for glutamylation. With the NH_4^+-N supply, HPPK-DHPS, DHFS, and DHFR activities were reduced by varying degrees, subject to a series of complex feedback regulation processes by folate or its synthesis intermediates, for instance, negative feedback of DHP and DHF on HPPK-DHPS, and 5-CHO-THF negative feedback on DHFR (Gorelova et al., 2017; Li et al., 2021).

The final reason for folate enhancement is the increased stability of folates. The extent of folate polyglutamylation, which is defined by the polyglutamylated tail length, can affect cellular folate breakdown to alter folate levels. The extent is determined by FPGS adding a Glu tail and GGH removing it. In tomatoes, the overexpression of GGH caused extensive

deglutamylation of polyglutamylated folates and resulted in a total folate content reduction of approximately 40%. In contrast, lower GGH activity in tomatoes was associated with an increased folate level (Akhtar et al., 2010; Tyagi et al., 2023). With NH_4^+-N application, GGH activity was significantly lower than that with NO_3^--N supply alone. Correspondingly, the higher polyglutamylated folate level with NH_4^+-N supply seems to be the result of reduced GGH activity, weakening the deglutamylation process. In addition to folate polyglutamylation, the folate form can affect folate breakdown. 5-CHO-THF is the most stable form among folates, followed by 5-CH_3-THF (Díaz de la Garza et al., 2019). The increase in total folate level with NH_4^+-N application was mainly due to the increase of polyglutamylated 5-CHO-THF, followed by polyglutamylated 5-CH_3-THF, of which 5-CHO-THF was dominant. Thus, the folates of the treatments with NH_4^+-N are more stable and less susceptible to degradation. 5-CHO-THF is the only derivative that does not function as a one-carbon donor while modulating C and N metabolism (Li et al., 2021). It is very likely that the increased 5-CHO-THF with the NH_4^+-N treatments regulated the change in C and N metabolism.

Enhanced folate accumulation means that more substances are consumed to support folate synthesis. In our study, most of the metabolites of C and N metabolism or folate synthesis showed a significant negative correlation with folate contents, which can be explained by the enhancement of folate biosynthesis by NH_4^+-N supply, increasing the consumption of these metabolites. Additionally, the significantly positive correlations between the activities of GTPCHI, ADCS, HPPK-DHPS, and DHFS and their respective substrates and products suggest that these enzymes may be the main control points for the increased metabolite consumption. Given that low GGH activity is conducive to enhanced folate synthesis, the significant negative correlation between GGH activity and folate contents indicates that low GGH activity is a key factor in the enhancement of folate biosynthesis with NH_4^+-N supply.

In conclusion, an appropriate NO_3^-/NH_4^+ ratio in nutrient solution could promote pakchoi growth and enhance the metabolic flux of C and N metabolism, especially with respect to glucose accumulation in shoots and folate biosynthesis. This therefore increases folate contents in pakchoi shoots, mainly in the form of polyglutamylated 5-CHO-THF and polyglutamylated 5-CH_3-THF. The rate of folate biosynthesis could be controlled by the activities of GTPCHI, ADCS, HPPK-DHPS, and DHFS. At the same N concentration, NH_4^+-N supply could increase polyglutamylated folates by reducing folate deglutamylation via lower GGH activity, which is conducive to folate stability. With good growth responses and folate biofortification, the appropriate 70/30 NO_3^-/NH_4^+ ratio in nutrient solution should be recommended for the hydroponic cultivation of pakchoi. For the optimal growth and efficient folate accumulation of other foliar vegetable crops under hydroponic conditions, the appropriate ratio of NH_4^+-N to NO_3^--N needs further exploration.

Data availability statement

All datasets analyzed in this study are available from the corresponding author upon request.

Acknowledgments

This work was supported by the Ministry of Agriculture and Rural Affairs of China Major Project for Support System Construction of Agriculture Green Development in Anji County (No. NG/LS2020-71-05).

Author contributions

Yongcong ZHU performed the experimental research and data analysis, and wrote and edited the manuscript. Wei CHENG performed the experimental research and data analysis. Yuemin NI contributed to the study design. Wuzhong NI contributed to the study design and writing and editing of the manuscript. All authors have read and approved the final manuscript, and therefore, have full access to all the data in the study and take responsibility for the integrity and security of the data.

Compliance with ethics guidelines

Yongcong ZHU, Wei CHENG, Yuemin NI, and Wuzhong NI declare that they have no conflicts of interest.

This article does not contain any studies with human or animal subjects performed by any of the authors.

References

Akhtar TA, Orsomando G, Mehrshahi P, et al., 2010. A central role for gamma-glutamyl hydrolases in plant folate homeostasis. *Plant J*, 64(2):256-266. https://doi.org/10.1111/j.1365-313X.2010.04330.x

Bailey LB, 1998. Dietary reference intakes for folate: the debut of dietary folate equivalents. *Nutr Rev*, 56(10):294-299. https://doi.org/10.1111/j.1753-4887.1998.tb01662.x

Bailey LB, Stover PJ, McNulty H, et al., 2015. Biomarkers of nutrition for development—folate review. *J Nutr*, 145(7):

1636S-1680S.
https://doi.org/10.3945/jn.114.206599

Blancquaert D, de Steur H, Gellynck X, et al., 2014. Present and future of folate biofortification of crop plants. *J Exp Bot*, 65(4):895-906.
https://doi.org/10.1093/jxb/ert483

Blancquaert D, van Daele J, Strobbe S, et al., 2015. Improving folate (vitamin B_9) stability in biofortified rice through metabolic engineering. *Nat Biotechnol*, 33(10):1076-1078.
https://doi.org/10.1038/nbt.3358

Boschiero BN, Mariano E, Azevedo RA, et al., 2019. Influence of nitrate-ammonium ratio on the growth, nutrition, and metabolism of sugarcane. *Plant Physiol Biochem*, 139: 246-255.
https://doi.org/10.1016/j.plaphy.2019.03.024

Delchier N, Herbig AL, Rychlik M, et al., 2016. Folates in fruits and vegetables: contents, processing, and stability. *Compr Rev Food Sci Food Saf*, 15(3):506-528.
https://doi.org/10.1111/1541-4337.12193

Díaz de la Garza RI, Ramos-Parra PA, Vidal-Limon HR, 2019. Biofortification of crops with folates: from plant metabolism to table. *In*: Jaiwal PK, Chhillar AK, Chaudhary D, et al. (Eds.), Nutritional Quality Improvement in Plants. Springer, Cham, p.137-175.
https://doi.org/10.1007/978-3-319-95354-0_6

Esteban R, Ariz I, Cruz C, et al., 2016. Review: mechanisms of ammonium toxicity and the quest for tolerance. *Plant Sci*, 248:92-101.
https://doi.org/10.1016/j.plantsci.2016.04.008

US Preventive Services Task Force, 2017. Folic acid supplementation for the prevention of neural tube defects: US Preventive Services Task Force recommendation statement. *JAMA*, 317(2):183-189.
https://doi.org/10.1001/jama.2016.19438

Gao HD, Yue XZ, Li ZT, et al., 2023. The molecular regulation of folate accumulation in pakchoi by low intensity white light-emitting diode (LED) illumination. *Sci Hortic*, 314:111937.
https://doi.org/10.1016/j.scienta.2023.111937

Gorelova V, Ambach L, Rébeillé F, et al., 2017. Folates in plants: research advances and progress in crop biofortification. *Front Chem*, 5:21.
https://doi.org/10.3389/fchem.2017.00021

Gräwert T, Fischer M, Bacher A, 2013. Structures and reaction mechanisms of GTP cyclohydrolases. *IUBMB Life*, 65(4):310-322.
https://doi.org/10.1002/iub.1153

Hachiya T, Sakakibara H, 2017. Interactions between nitrate and ammonium in their uptake, allocation, assimilation, and signaling in plants. *J Exp Bot*, 68(10):2501-2512.
https://doi.org/10.1093/jxb/erw449

Hanson AD, Gregory III JF, 2011. Folate biosynthesis, turnover, and transport in plants. *Annu Rev Plant Biol*, 62: 105-125.
https://doi.org/10.1146/annurev-arplant-042110-103819

He YN, Song SH, Li C, et al., 2022. Effect of germination on the main chemical compounds and 5-methyltetrahydrofolate metabolism of different quinoa varieties. *Food Res Int*, 159:111601.
https://doi.org/10.1016/j.foodres.2022.111601

Kołton A, Długosz-Grochowska O, Wojciechowska R, et al., 2022. Biosynthesis regulation of folates and phenols in plants. *Sci Hortic*, 291:110561.
https://doi.org/10.1016/j.scienta.2021.110561

Krapp A, 2015. Plant nitrogen assimilation and its regulation: a complex puzzle with missing pieces. *Curr Opin Plant Biol*, 25:115-122.
https://doi.org/10.1016/j.pbi.2015.05.010

Lee KT, Liao HS, Hsieh MH, 2023. Glutamine metabolism, sensing and signaling in plants. *Plant Cell Physiol*, 64(12): 1466-1481.
https://doi.org/10.1093/pcp/pcad054

Li WC, Liang QJ, Mishra RC, et al., 2021. The 5-formyltetrahydrofolate proteome links folates with C/N metabolism and reveals feedback regulation of folate biosynthesis. *Plant Cell*, 33(10):3367-3385.
https://doi.org/10.1093/plcell/koab198

Lian T, Wang XX, Li S, et al., 2022. Comparative transcriptome analysis reveals mechanisms of folate accumulation in maize grains. *Int J Mol Sci*, 23(3):1708.
https://doi.org/10.3390/ijms23031708

Liu Y, von Wirén N, 2017. Ammonium as a signal for physiological and morphological responses in plants. *J Exp Bot*, 68(10):2581-2592.
https://doi.org/10.1093/jxb/erx086

Nakamichi Y, Kobayashi J, Toyoda K, et al., 2023. Structural basis for the allosteric pathway of 4-amino-4-deoxychorismate synthase. *Acta Crystallogr D Struct Biol*, 79:895-908.
https://doi.org/10.1107/S2059798323006320

Patrick JW, Botha FC, Birch RG, 2013. Metabolic engineering of sugars and simple sugar derivatives in plants. *Plant Biotechnol J*, 11(2):142-156.
https://doi.org/10.1111/pbi.12002

Ramos-Parra PA, Urrea-López R, Díaz de la Garza RI, 2013. Folate analysis in complex food matrices: use of a recombinant Arabidopsis γ-glutamyl hydrolase for folate deglutamylation. *Food Res Int*, 54:177-185.
https://doi.org/10.1016/j.foodres.2013.06.026

Saini RK, Nile SH, Keum YS, 2016. Folates: chemistry, analysis, occurrence, biofortification and bioavailability. *Food Res Int*, 89:1-13.
https://doi.org/10.1016/j.foodres.2016.07.013

Scaglione F, Panzavolta G, 2014. Folate, folic acid and 5-methyltetrahydrofolate are not the same thing. *Xenobiotica*, 44(5):480-488.
https://doi.org/10.3109/00498254.2013.845705

Tyagi K, Sunkum A, Gupta P, et al., 2023. Reduced γ-glutamyl hydrolase activity likely contributes to high folate levels in Periyakulam-1 tomato. *Hortic Res*, 10:284-296.
https://doi.org/10.1093/hr/uhac235

Wan X, Han LD, Yang M, et al., 2019. Simultaneous extraction and determination of mono-/polyglutamyl folates using high-performance liquid chromatography-tandem mass spectrometry and its applications in starchy crops. *Anal Bioanal Chem*, 411(13):2891-2904.
https://doi.org/10.1007/s00216-019-01742-0

Wang M, Shen QR, Xu GH, et al., 2014. New insight into the strategy for nitrogen metabolism in plant cells. *Int Rev Cell Mol Biol*, 310:1-37. https://doi.org/10.1016/B978-0-12-800180-6.00001-3

Wang Y, Wang JS, Dong EW, et al., 2023. Foxtail millet [*Setaria italica* (L.) P. Beauv.] grown under nitrogen deficiency exhibits a lower folate contents. *Front Nutr*, 10:1035739. https://doi.org/10.3389/fnut.2023.1035739

Watanabe S, Ohtani Y, Tatsukami Y, et al., 2017. Folate biofortification in hydroponically cultivated spinach by the addition of phenylalanine. *J Agric Food Chem*, 65(23): 4605-4610. https://doi.org/10.1021/acs.jafc.7b01375

Xu GH, Fan XR, Miller AJ, 2012. Plant nitrogen assimilation and use efficiency. *Annu Rev Plant Biol*, 63:153-182. https://doi.org/10.1146/annurev-arplant-042811-105532

Yokoyama R, Kleven B, Gupta A, et al., 2022. 3-Deoxy-D-arabino-heptulosonate 7-phosphate synthase as the gatekeeper of plant aromatic natural product biosynthesis. *Curr Opin Plant Biol*, 67:102219. https://doi.org/10.1016/j.pbi.2022.102219

Supplementary information

Table S1